Hydration and Raman scattering studies of levitated microparticles: $Ba(NO_3)_2$, $Sr(NO_3)_2$, and $Ca(NO_3)_2$

I. N. Tang and K. H. Fung
Environmental Chemistry Division, Department of Applied Science, Brookhaven National Laboratory, Upton, New York 11973

(Received 13 August 1996; accepted 25 October 1996)

The phase transformation and hydration of inorganic salt particles composed of alkaline earth metal nitrates, $Ba(NO_3)_2$, $Sr(NO_3)_2$, and $Ca(NO_3)_2$, are investigated in a quadrupole cell, in which a levitated single microparticle is in dynamic equilibrium with water vapor under controlled humidity conditions. Laser Raman and Mie scattering techniques are used to probe the chemical and physical states of the microparticle before and after phase transformation. Because of the high degree of supersaturation that only a suspended solution droplet can attain before solidifying, metastable states not predicted from bulk solution thermodynamics often result. Thus it is found that, except for $Ba(NO_3)_2$ particles which form the stable anhydrous crystalline state upon efflorescence, $Sr(NO_3)_2$ and $Ca(NO_3)_2$ droplets solidify to a metastable amorphous state that contains residual water persisting even in high vacuum. Raman spectra of the amorphous particles reveal that the nitrate ions form contact-ion pairs with the bivalent cations and that the residual water molecules possess very little, if any, hydrogen bond characteristics. The deliquescence properties of the amorphous particles, which are found to be different from those expected of the bulk crystalline states, are also reported. © *1997 American Institute of Physics.* [S0021-9606(97)51605-9]

INTRODUCTION

In recent years, experimental methods developed for trapping a single micron-sized particle in a stable optical or electrical potential cavity have made it possible to study many physical and chemical properties of microparticles. These properties are either unique to small particles or otherwise inaccessible to measurement with bulk samples. An earlier review by Davis[1] documented the progress up to 1982. Since then, many interesting investigations have appeared in the literature. In particular, thermodynamic[2–7] and optical properties[8] of electrolyte solutions at concentrations far beyond saturation that could not have been achieved in the bulk, can now be measured with a suspended droplet. This is accomplished by continuously monitoring the changes in weight and in Mie scattering patterns of a single suspended solution droplet undergoing growth or evaporation in a humidity-controlled atmosphere, thus providing extensive information over the entire concentration region. Other interesting studies on the physics and chemistry of microparticles are also discussed in another recent review by Davis.[9] In addition, experimental techniques have been developed to characterize the physical and chemical state of suspended single microparticles by Raman spectroscopy.[10–14]

Since the early 1960's when lasers became easily accessible as the source of excitation, a large amount of work has been done to elucidate the structure of electrolyte solutions by vibrational spectroscopy. Comprehensive reviews of infrared and Raman studies of electrolytes were presented in 1976 by Irish and Brooker,[15] and again in 1986 by Brooker.[16] Much of the impetus for Raman spectral studies of aqueous solutions has been the search for ion-hydrates, ion-pairs, and other discrete species that have been invoked in the earlier models for explaining thermodynamic and electrochemical measurements. In particular, because of the great potential of the nitrate ion pairing with the doubly charged cations in solutions, aqueous alkaline earth metal nitrate solutions have received special attention. Consequently, much progress has been made to date.

In the present work, hydration experiments, in conjunction with Raman and Mie resonance spectroscopy, were conducted specifically to study the phase transformation and solution properties of aqueous droplets containing alkaline earth metal nitrates. Because of the high degree of supersaturation that only solution droplets can attain before solidifying, metastable states not predicted from bulk solution thermodynamics often result.[17] An understanding of the structures and properties of these metastable amorphous states should provide further insights into the ion–ion and ion–solvent interactions that occur in solution droplets at high concentrations otherwise inaccessible with bulk solutions.

EXPERIMENT

Single particle levitation is achieved in a quadrupole cell (or electrodynamic balance) that has been described elsewhere.[8,10] Briefly, an electrostatically charged particle, 14–16 μm in diameter, is trapped at the null point of the cell by an ac field imposed on a ring electrode surrounding the particle. The particle is balanced against gravity by a dc potential established between two endcap electrodes positioned symmetrically above and below the particle. All electrode surfaces are hyperboloidal in shape and separated by Teflon insulators. The quadrupole cell is housed in a high vacuum system that can be evacuated to a pressure below 10^{-7} Torr. A schematic diagram of the experimental set-up is shown in Fig. 1.

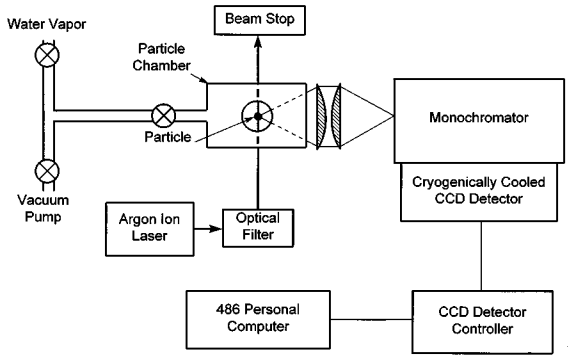

FIG. 1. A schematic diagram of the apparatus for hydration and Raman scattering studies of a levitated microparticle.

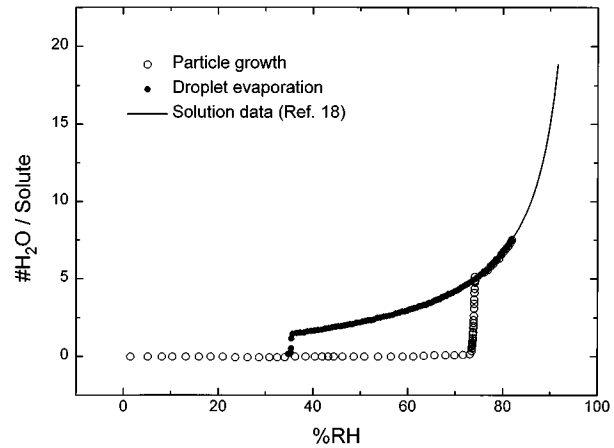

FIG. 2. Growth and evaporation of a $NaNO_3$ particle.

In particle hydration studies, a vertically polarized He–Ne laser is used to illuminate the particle. The particle position is continuously monitored by a CCD video camera and displayed on a monitor for precise null point balance. The change in the dc voltage used to balance the particle in the null point during droplet growth or evaporation is a direct measure of the particle mass change. The 90° scattered light is also continuously monitored with a photomultiplier tube. The laser beam, which is modulated by a chopper, is focused on the particle so that a lock-in amplifier can be used to achieve the high signal-to-noise ratio required in the Mie scattering measurement. Initially, a filtered solution of known composition is loaded in a particle gun; a charged particle is injected into the cell and captured in dry nitrogen at the center of the cell by properly manipulating the ac and dc voltages applied to the electrodes. The system is closed and evacuated to a pressure below 10^{-6} Torr. The vacuum is then valved off and the dc voltage required to position the particle at the null point is noted. The system is then slowly back filled with water vapor during particle deliquescence and growth. Conversely, the system is gradually evacuated during droplet evaporation and efflorescence. The water vapor pressures and the balancing dc voltages at prescribed time intervals are simultaneously recorded in pairs during the entire experiment, thus enabling the water activity and solute mass fraction at any given point to be determined. The measurements can be repeated several times with the same particle by simply repeating the growth and evaporation cycle. The reproducibility is better than ±2%.

A typical hydration experiment performed with a deliquescent $NaNO_3$ particle is illustrated in Fig. 2. Here, the particle mass change resulting from either water vapor condensation (shown as open circles) or evaporation (shown as filled circles) is expressed as moles of water per mole of solute ($\sharp H_2O$/solute) and plotted as a function of relative humidity (%RH). Thus as %RH increases, a solid $NaNO_3$ particle remains unchanged until at 74.5 %RH when it deliquesces spontaneously to form a saturated solution droplet containing about 5 $\sharp H_2O$/solute. The droplet continues to grow as %RH further increases. The solid line in the figure represents the solution data taken from the tabulation by Robinson and Stokes.[18] Upon evaporation, the solution droplet passes the deliquescence point without phase change and becomes highly supersaturated as a metastable droplet. Finally, crystallization occurs at about 35 %RH. Note that, in a bulk solution, crystallization always takes place not far beyond the saturation point. This happens because the presence of dust particles and the container walls invariably induces heterogeneous nucleation long before homogeneous nucleation finally sets in as in a solution droplet. The hysteresis loop shown in Fig. 2 illustrates a typical behavior exhibited by deliquescent aerosol particles.[19,20]

In Raman scattering studies, the same particle that is being levitated in the quadrupole cell for the hydration experiment is now excited by the 5145 Å line of an argon-ion laser (Coherent Innova-400). Referring back to the schematic diagram shown in Fig. 1, the polarization of the laser beam is set to be perpendicular to the scattering plane. A 10 cm focal length lens focuses the laser beam from the bottom of the cell onto the particle with a nominal power of 500 mW. The scattered light is collected with a condenser lens and is imaged onto the entrance slit of the monochromator. The light collecting optics are optimized at $f/1$ and set to match the f-number of the monochromator. The setting of the monochromator slit width is determined by the projected image size and the optimal resolution. The photon detection system is a cryogenically cooled CCD detector (SPEX Industries, NJ). For a typical spectrum, the total exposure time of the detector is about 20 s. Optical scattering spectra are transferred by a DMA interface board to a 486-based computer where the data are displayed, stored, and later analyzed. The monochromator is routinely calibrated against the neon spectrum. Owing to the five- to sevenfold magnification in the imaging optics for optimal photon collection and spectral resolution, the entrance slit of the monochromator must be increased in order to accommodate the projected particle image size. As a result, the practical resolution is reduced. Two monochromators are used in the experiments. For high resolution, a 0.75 m double monochromator (SPEX 1403) with an ultimate resolution of 0.1 cm^{-1} is chosen, which actually delivers a practical resolution of 1 cm^{-1} and a coverage of 200 cm^{-1} per CCD exposure. For a wider spectral coverage, a combi-

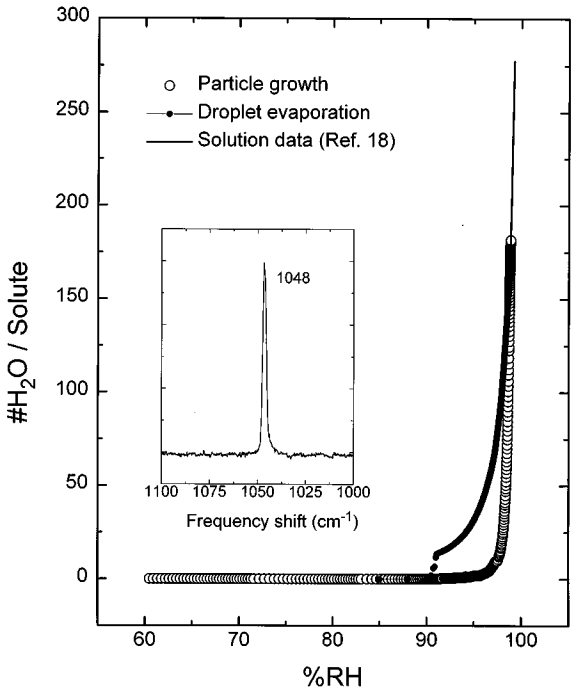

FIG. 3. Growth and evaporation of a $Ba(NO_3)_2$ particle. The inset is the nitrate ν_1 mode in the Raman spectra taken of the crystalline anhydrous particle both before deliquescence and after crystallization.

nation of a 0.64 m single monochromator (ISA HR-640) and a high rejection holographic bandpass filter (Physical Optics Corp., CA) is used. The coverage is about 650–750 cm^{-1} depending on the excitation laser. The practical resolution of this single monochromator is about 4 cm^{-1}, although the ultimate resolution is in the order of 1 cm^{-1}.

Either reagent grade or puratonic grade chemicals were used without further purification. Water was obtained from a Millipore super Q ultra pure water system and had a specific resistance of >18 MΩ cm.

RESULTS AND DISCUSSION

$Ba(NO_3)_2$ particles

$Ba(NO_3)_2$ is not very soluble in water, with a solubility[21] of 8.27 g/100 g solution at 20 °C, corresponding to 161 $\sharp H_2O$/solute. Thus when an anhydrous particle deliquesces, it will grow about 12 times its dry mass by water vapor condensation. The hydration behavior of a $Ba(NO_3)_2$ particle at 17.8 °C is shown in Fig. 3. During growth, the particle deliquesced at 98.8 %RH to form a saturated solution droplet at about 175 $\sharp H_2O$/solute. Upon evaporation, the droplet was observed to crystallize at 91 %RH, when the concentration reached about 13.6 $\sharp H_2O$/solute, which is about 13 times the saturation concentration of its bulk solution. Despite the extremely high supersaturation at which the droplet crystallized, the resulting solid particle was in the anhydrous crystalline state as the original particle. This was confirmed by both the mass measurement and the Raman spectrum taken of the particle after its crystallization. The symmetric stretch $\nu_1(A_1')$ mode of the nitrate ion in the particle, shown in the inset of Fig. 3 as the narrow band at 1048 cm^{-1} Raman frequency shift, is identical to that of the anhydrous $Ba(NO_3)_2$ powders.[22] The hydration behavior of $Ba(NO_3)_2$ particles is qualitatively similar to that of $NaNO_3$ particles. It is, however, remarkable that $Ba(NO_3)_2$ droplets sustain such a high degree of supersaturation before crystallization finally takes place.

TABLE I. Standard free energy of formation values.

Compound	ΔG_f^0 (kJ/mol)
$H_2O(g)$	−228.593
$Sr(NO_3)_2(c)$	−780.15
$Sr(NO_3)_2\cdot 4H_2O(c)$	−1730.71
$Ca(NO_3)_2(c)$	−743.20
$Ca(NO_3)_2\cdot 4H_2O(c)$	−1713.47

$Sr(NO_3)_2$ particles

Preliminary results on the hydration behavior of $Sr(NO_3)_2$ particles have been reported.[17] Solubility data[21] indicate that below 29.3 °C the solid phase in equilibrium with the saturated solution is the crystalline tetrahydrate, $Sr(NO_3)_2\cdot 4H_2O$. In fact, dry tetrahydrate crystals readily decompose at room temperatures to form the anhydrous state. The relative stability of the two solid states may be estimated from a consideration of the standard Gibb's free energy change, $\Delta \mathbf{G}^0$, of the system

$$Sr(NO_3)_2(c)+4H_2O(g)=Sr(NO_3)_2\cdot 4H_2O(c)$$

so that,

$$\Delta \mathbf{G}^0=\Delta \mathbf{G}_f^0[Sr(NO_3)_2\cdot 4H_2O(c)]-\Delta \mathbf{G}_f^0[Sr(NO_3)_2(c)]-4\Delta \mathbf{G}_f^0[H_2O(g)]$$

$$\Delta \mathbf{G}^0=-RT\ \ln(1/p^4). \quad (1)$$

Here, c and g in the parentheses refer to the crystalline state and gas phase, respectively, R is the gas constant, T is the absolute temperature, and p is the equilibrium water vapor pressure. $\Delta \mathbf{G}^0$ may be evaluated from the tabulated[23] values of standard free energy of formation, $\Delta \mathbf{G}_f^0$, as given in Table I. A value of −36.19 kJ/mol is obtained for $\Delta \mathbf{G}^0$. Using Eq. (1), p is then calculated to be 19.75 Torr, or 83.1 %RH at 25 °C. Thus the tetrahydrate is only stable above 83 %RH.

The hydration behavior of a certain $Sr(NO_3)_2$ particle, as shown in Fig. 4(a), is rather interesting. Starting out as an anhydrous particle, upon growth (shown as open circles), it deliquesced right at 83 %RH, instead of following the predicted pathways (shown as dashed lines) first to transform into the tetrahydrate state and then to deliquesce at 85 %RH. In fact, all anhydrous $Sr(NO_3)_2$ particles were observed not to follow the pathways predicted by equilibrium thermodynamics. During evaporation (shown as filled circles), the particle remained a supersaturated solution droplet until at 60 %RH when it abruptly solidified. However, in most cases as this one, the particle did not return to the anhydrous state, but rather became an amorphous solid that consistently and te-

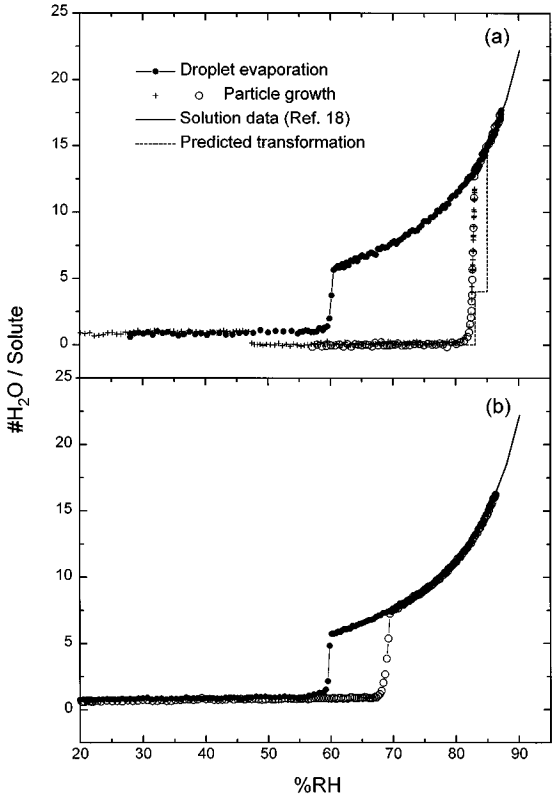

FIG. 4. Growth and evaporation of (a) an anhydrous particle, and (b) an amorphous particle of $Sr(NO_3)_2$.

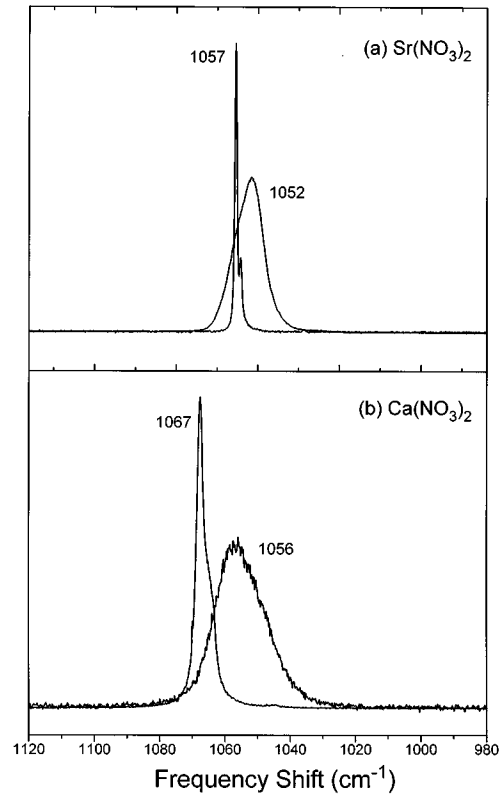

FIG. 5. Comparison of the nitrate ν_1 mode in the Raman spectra between anhydrous and amorphous states of (a) $Sr(NO_3)_2$ and (b) $Ca(NO_3)_2$ particles.

naciously held about 1 $\sharp H_2O$/solute even in vacuum. When %RH was raised again, an amorphous particle would slightly pick up some water and then deliquesce at 69 %RH as shown in Fig. 4(b). Occasionally, there are exceptions to this rule, such as the particle shown in Fig. 4(a). It revealed its metastable characteristics by completely shedding its water content to transform into an anhydrous particle, even during growth (shown as crosses) in this case at about 47 %RH, and then proceeded to deliquesce at 83 %RH.

As shown in Fig. 5(a), the $\nu_1(A_1')$ band of the nitrate ion in the amorphous $Sr(NO_3)_2$ particle appears rather broad at 1052 cm^{-1}, in contrast to the narrow bands at 1057 and 1055 cm^{-1} in an anhydrous particle [which, within experimental errors, agree with the 1055.6 and 1054.4 cm^{-1} bands in powdered $Sr(NO_3)_2$ sample[22]]. A comprehensive Raman spectral study of the aqueous $Sr(NO_3)_2$ solutions at various concentrations was made in 1950 by Mathieu and Lounsbury,[24] and again in 1975 by Bulmer *et al.*[25] In general, a hydrated or free nitrate ion, having a plane structure in the form of a centered equilateral triangle and belonging to the point group D_{3h}, is known[25] to have fundamental vibrational frequencies at 1049 $\nu_1(A_1')$, 830 $\nu_2(A_2'')$, ~1354 and ~1410 $\nu_3(E')$, 718 $\nu_4(E')$, and 1660 cm^{-1} $2\nu_2$. The out-of-plane bending mode ν_2 is Raman forbidden and is not observed in dilute solutions. Figure 6(a) shows the Raman spectrum of $Sr(NO_3)_2$ solution at 15 $\sharp H_2O$/solute, revealing most features just described. However, a new peak at 732 cm^{-1} is observed to emerge, which is attributed[25] to the formation of ion pairs in

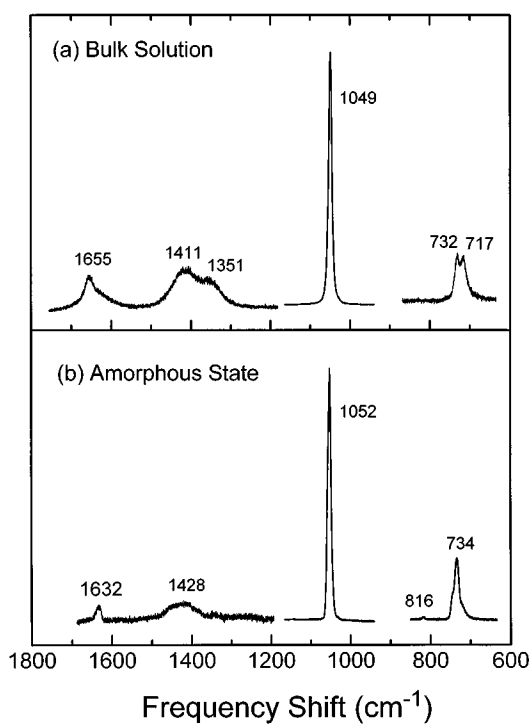

FIG. 6. Comparison of Raman spectra of the nitrate ion between (a) in the bulk solution and (b) in amorphous particle for $Sr(NO_3)_2$ over all vibration modes.

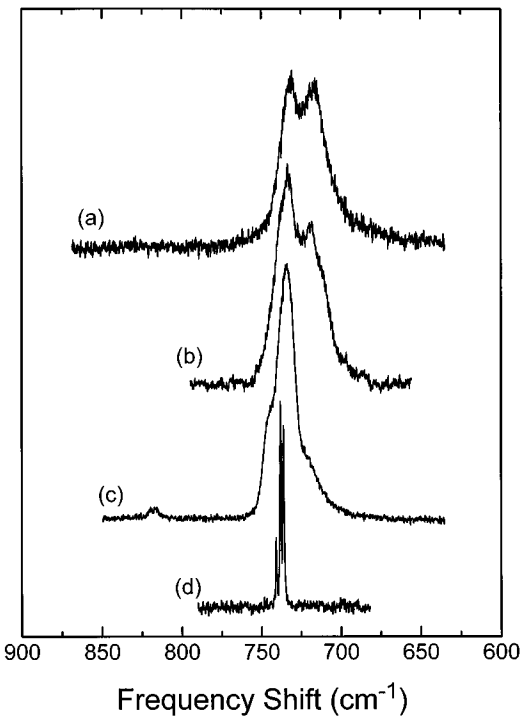

FIG. 7. Comparison of the ν_4 mode in the Raman spectra of the nitrate group present in various environments: (a) solution at 15 $\sharp H_2O$/solute, (b) droplet at 10 $\sharp H_2O$/solute, (c) amorphous particle at ca. 1 $\sharp H_2O$/solute, (d) anhydrous particle.

concentrated solutions. In comparison, the Raman spectrum of the amorphous state is shown in Fig. 6(b). The two spectra are qualitatively similar, but the corresponding peak positions are slightly shifted from each other. The most striking feature is the predominant appearance of the 734 cm^{-1} peak at the expense of the 717 cm^{-1} peak, indicating that in the amorphous state the nitrate ion is in constant association with the cation. The ν_2 mode appearing at 816 cm^{-1} is now no longer Raman forbidden, as the nitrate ion becomes bound to the cation and thus belongs to a lower symmetry group C_{2v}. Fleissner *et al.*[26] have recently used the ν_2 band in the FTIR spectra of $LiNO_3$ and $Ca(NO_3)_2$ solutions in D_2O as an indicator for contact-ion pairing in aqueous nitrate solutions.

The various states of the nitrate ion in different environments are lucidly illustrated in Fig. 7 again by the deformation mode ν_4. Spectrum (a) is the solution at 15 $\sharp H_2O$/solute showing the emergence of the bound nitrate ion at 732 cm^{-1} from the free nitrate ion at 717 cm^{-1}. More bound species at 733 cm^{-1} is present in the supersaturated solution droplet at 10 $\sharp H_2O$/solute as shown in (b). In the amorphous state containing about 1 $\sharp H_2O$/solute, as shown in (c), the bound species at 734 cm^{-1} is predominant but the residual water stands in the way of allowing crystal lattices to form. Since the amorphous state deliquesces at a specific relative humidity (69 %RH), it is not a continuation of the aqueous solution. When the residual water is finally removed, an anhydrous crystalline state is formed whose Raman spectrum is shown in (d) with narrow peaks at 736, 738, and 741 cm^{-1}. The correlation field splitting of the ν_4 band due to vibrational coupling within the crystallographic unit cell has been fully described by Brooker *et al.*[22] As discussed earlier, an anhydrous crystalline particle deliquesces at 83 %RH, which is quite different from the deliquescence relative humidity, 69 %RH, of the amorphous particles.

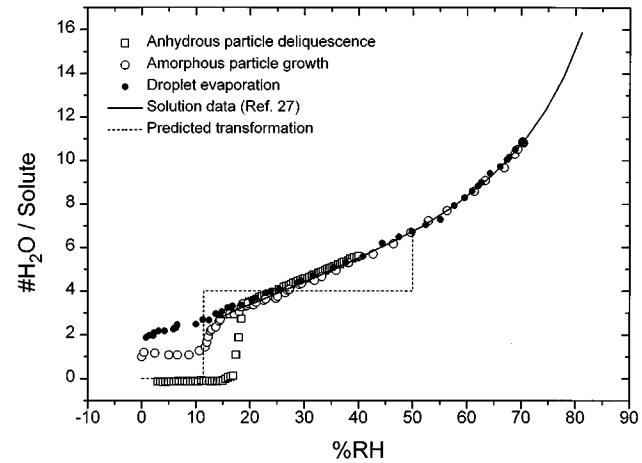

FIG. 8. Growth and evaporation of $Ca(NO_3)_2$ particles.

$Ca(NO_3)_2$ particles

Stokes and Robinson[27] have made isopiestic measurements on highly concentrated $Ca(NO_3)_2$ solutions. While the solution is saturated at 6.6 $\sharp H_2O$/solute at 25 °C, it readily supersaturates even in the bulk phase up to 2.8 $\sharp H_2O$/solute. Upon concentration by isothermal evaporation, the supersaturated solutions pass from freely flowing liquids into clear semisolid gels. The transition is marked by no visible discontinuity and the vapor pressure-concentration curve is also continuous. Solution thermodynamics[21] indicates that the tetrahydrate $Ca(NO_3)_2 \cdot 4H_2O$ is the solid phase in equilibrium with the saturated solution. Unlike the strontium salt, $Ca(NO_3)_2 \cdot 4H_2O$ is stable in air up to its congruent melting point 42.7 °C. Using Eq. (1) and the appropriate ΔG_f^0 values given in Table I, the relative stability of the tetrahydrate and the anhydrous salts can be estimated. An equilibrium water vapor pressure 2.71 Torr at 25 °C is obtained, indicating that an anhydrous particle would transform into the tetrahydrate state at 11.4 %RH, which would then deliquesce to form a saturated solution droplet at 50 %RH.[18]

The hydration behavior of the $Ca(NO_3)_2$ particles is shown in Fig. 8. Instead of transforming into the tetrahydrate at 11.4 %RH, the anhydrous particle deliquesces at the higher humidity 18 %RH to become a supersaturated solution droplet. In fact, the stable tetrahydrate state has never been observed to exist in a microparticle. Once in solution, the droplet grows and evaporates following the curve derived from isopiestic measurements with bulk solutions, as shown by the solid line in Fig. 8. Upon further evaporation, the saturated solution droplet continues to lose water until in vacuum it turns into an amorphous particle containing 1 $\sharp H_2O$/solute. Mie scattering data indicate that the amorphous $Ca(NO_3)_2$ particle maintains its spherical shape. Neverthe-

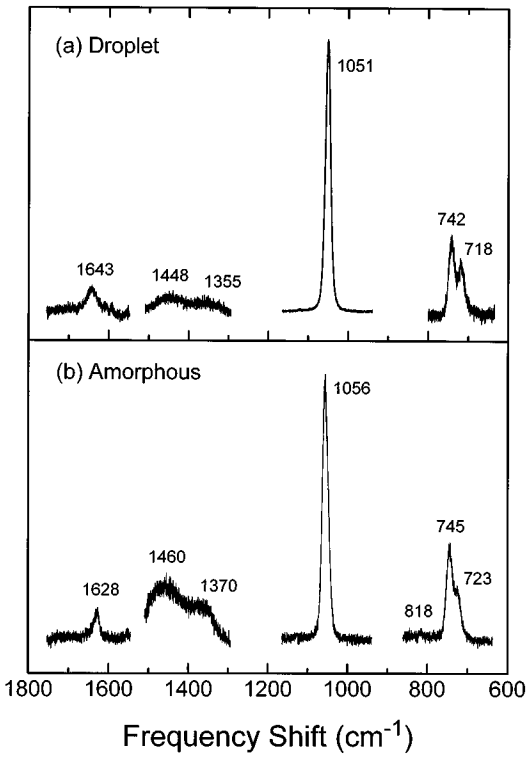

FIG. 9. Comparison of Raman spectra of the nitrate ion between (a) in supersaturated solution droplet and (b) in amorphous particle for $Ca(NO_3)_2$ over all vibration modes.

less, it deliquesces at ~13 %RH, indicating that it is not a continuation of the supersaturated solution droplet, but rather a new phase formed by "freezing over" from the highly supersaturated solution droplet.

As shown in Fig. 5(b), the $\nu_1(A_1')$ band of the nitrate ion in the amorphous $Ca(NO_3)_2$ particle again appears rather broad at 1056 cm^{-1}, in contrast to the narrow band at 1067 and a shoulder at 1065 cm^{-1} in an anhydrous particle [which, within experimental errors, agree with the 1069.3 and 1066.2 cm^{-1} bands in powdered $Ca(NO_3)_2$ sample[22]]. On the other hand, the similarities are remarkable between the Raman spectrum of a supersaturated solution droplet containing 5 $\sharp H_2O$/solute, as shown in Fig. 9(a), and that of the amorphous particle containing 1 $\sharp H_2O$/solute, as shown in Fig. 9(b). In particular, the prominent band at 745 cm^{-1} of the amorphous particle may be compared to the 742 cm^{-1} band of the solution droplet to infer the predominant presence[28] of the contact-ion pair, $CaNO_3^+$. The ν_2 band at 818 cm^{-1} has also appeared to indicate extensive contact-ion pairing in the amorphous particle.

Because of the extremely high supersaturation that $Ca(NO_3)_2$ solutions can achieve in the bulk phase, they offer a good opportunity to investigate ion association in concentrated solutions using vibrational spectroscopy. Many studies have been done; more quantitative works are due to Hester and Plane[29] and Irish and Walrafen.[30] The monograph by Marcus[31] on ion solvation contains a comprehensive review chapter on solvation of ion pairs. The equilibrium constant for the association reaction

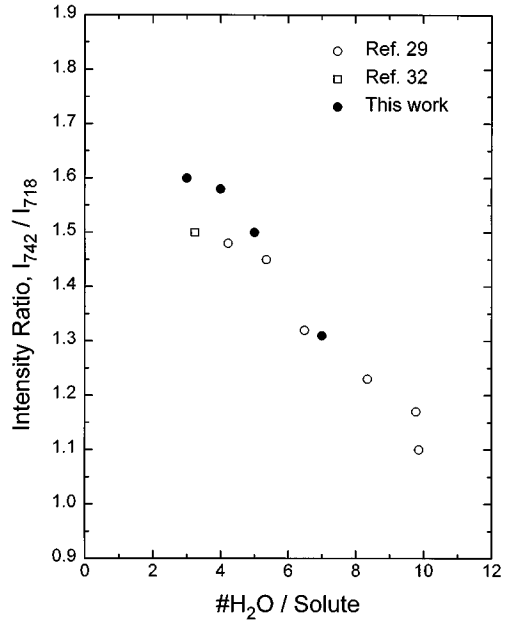

FIG. 10. Measured intensity ratio, I_{742}/I_{718}, as a function of concentration in solutions and droplets.

$$Ca^{++}+NO_3^- = CaNO_3^+$$

is given by

$$K_{assoc}=[CaNO_3^+]/[NO_3^-][Ca^{++}]. \tag{2}$$

Here, according to Hester and Plane,[29] the concentration ratio, $X=[CaNO_3^+]/[NO_3^-]$, is related to the Raman intensity ratio, I_{742}/I_{718}, through the expression

$$X=\frac{k_f}{k_b}\frac{I_{742}}{I_{718}} \tag{3}$$

and the unassociated cation concentration is given by

$$[Ca^{++}]=\frac{m_0}{2}\frac{(1-X)}{(1+X)}, \tag{4}$$

where k_b and k_f are the intrinsic molal scattering factors for the single lines 742 and 718 cm^{-1} characterizing bound and free nitrate ions, respectively, and m_0 is the total nitrate concentration in molality. A value of $k_f/k_b=0.365$ was reported by Hester and Plane.[29]

The Raman intensity ratio data, obtained with supersaturated solution droplets at different concentrations, are plotted in Fig. 10, together with the solution data reported by Hester and Plane.[29] Balshaw and Smedley[32] have reported the pressure dependence and their value at 1 bar is also shown in Fig. 10. All data points are seen to be in agreement within the experimental errors. A value of 0.161 ± 0.020 is obtained as the average of the K_{assoc} values computed from the data points, using Eqs. (2)–(4) and $k_f/k_b=0.365$. It is interesting to note that this K_{assoc} value is consistent with the equilibrium constants derived for other bivalent cations (e.g., 0.178 ±0.012 for $MgCl^+$) from indirect measurement techniques such as solution conductance measurements, as reported in the literature.[33]

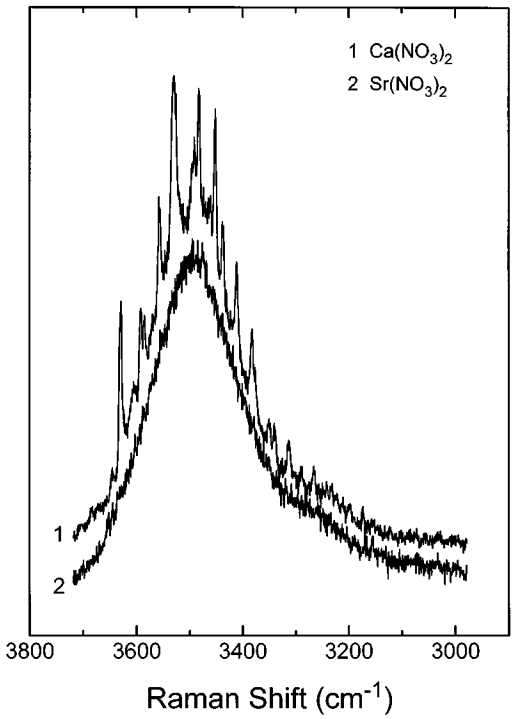

FIG. 11. Comparison of the OH stretch region in the Raman spectra of the residual water between amorphous $Ca(NO_3)_2$ and $Sr(NO_3)_2$ particles.

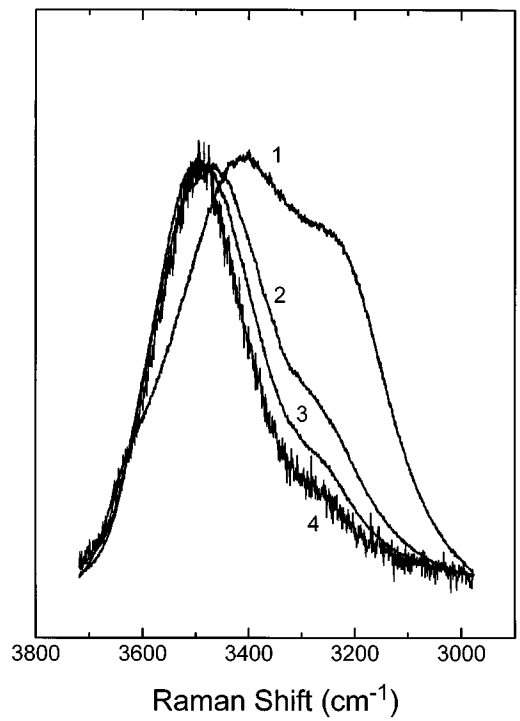

FIG. 12. Comparison of the OH stretch region in the Raman spectra of water present in various environments. 1- pure water; 2- $Ca(NO_3)_2$ solution at 9 $\sharp H_2O$/solute; 3- $Ca(NO_3)_2$ solution at 5 $\sharp H_2O$/solute; 4- amorphous $Sr(NO_3)_2$ particle at ca. 1 $\sharp H_2O$/solute.

The residual water

The Raman spectra of the OH stretching region of the residual water in the amorphous particles are shown in Fig. 11 for both $Sr(NO_3)_2$ and $Ca(NO_3)_2$. The sharp peaks superimposed on the Raman profile of the $Ca(NO_3)_2$ particle are Mie structure resonances[34] arising from the intensity enhancement when the wavelength of the scattered Raman light corresponds to the resonance conditions of the dielectric spherical particle. The occurrence of the Mie structure resonances is a positive indication that the amorphous $Ca(NO_3)_2$ particle is a homogeneous sphere. In contrast, the $Sr(NO_3)_2$ particle is not. Despite the difference in the physical shape, the structure of the residual water in both particles appears to be identical, as revealed by the remarkable similarity in the Raman profiles shown in Fig. 11 for the two amorphous particles.

A comparison of the OH stretching Raman profiles is also shown in Fig. 12 for the amorphous particle, solutions, and pure liquid water at 22 °C. Despite numerous spectroscopic and other studies reported in the literature, there is still no clear consensus as to the structure of liquid water.[35,36] Controversy has raged over what type of molecular model is to be adopted for liquid water. The two extremes may be classified broadly as the ''mixture'' models, describing water as an equilibrium mixture of clustered water molecules with varying numbers of hydrogen bonds, and the ''continuum'' models, describing water as an essentially complete hydrogen-bonded network with a distribution of hydrogen bond energies and geometries. It is generally observed,[37,38] however, that the higher frequency bands (nonhydrogen bond) in the OH stretching region increase in relative intensity while the lower frequency bands (hydrogen bond) decrease in relative intensity with temperature increase or/and electrolyte addition. The solute effects are adequately illustrated in Fig. 12. The profiles also bear good resemblance to the temperature effects on pure liquid water, as studied by many other investigators.[36,39] Regardless of the model, the changes in the spectra reflect the view that, in general, hydrogen bonding becomes less extensive as temperature or solute concentration increases. In the case of amorphous particles, which contain only one or less $\sharp H_2O$/solute, the frequency shifts and the relative intensity, as depicted in Fig. 12 for the amorphous particle, should represent the asymptotic values for water molecules still present as the solvent but seldom in close proximity of each other.

CONCLUSION

Bivalent alkaline-earth metal nitrates, $Sr(NO_3)_2$ and $Ca(NO_3)_2$, are found to form amorphous metastable states in hygroscopic microparticles. The presence of residual water is a prerequisite in the formation of the amorphous state. As soon as water is completely removed, an anhydrous crystalline particle always results. The metastable states exhibit hydration properties not predicted from bulk-phase thermodynamics. Raman spectral studies reveal that, while the free nitrate ion in the amorphous particles appears to resemble its presence in the supersaturated solution, being mostly associated with the cation as contact-ion pair, the residual water molecules are not in close proximity of each other, showing

little hydrogen-bond characteristics. Thus microparticles not only provide a means for studying some fundamental properties not easily accessible with bulk samples, but may also possess other unique and interesting properties not found in the bulk phase. The ubiquitous and abundant presence of microparticles both in the environment and in industrial processes merits continuing studies of the chemical and physical properties of these microparticles.

ACKNOWLEDGMENTS

We thank H. R. Munkelwitz for assistance in setting up the single-particle levitation apparatus and in performing some of the hydration experiments. This research was performed under the auspices of the U.S. Department of Energy under Contract No. DE-AC02-76CH00016.

[1] E. J. Davis, Aerosol Sci. Technol. **2**, 121 (1983).
[2] I. N. Tang and H. R. Munkelwitz, J. Colloid Interface Sci. **98**, 430 (1984).
[3] C. B. Richardson and J. F. Spann, J. Aerosol Sci. **15**, 563 (1984).
[4] C. B. Richardson and C. A. Kurtz, J. Am. Chem. Soc. **106**, 6615 (1984).
[5] I. N. Tang, H. R. Munkelwitz, and N. Wang, J. Colloid Interface Sci. **114**, 409 (1986).
[6] M. D. Cohn, R. C. Flagan, and J. H. Seinfeld, J. Phys. Chem. **91**, 4563 (1987).
[7] C. K. Chan, R. C. Flagan, and J. H. Seinfeld, Atmos. Environ. A **26**, 1661 (1992).
[8] (a) I. N. Tang and H. R. Munkelwitz, Aerosol Sci. Technol. **15**, 201 (1991); (b) J. Geophys. Res. **99**, 18,801 (1994).
[9] E. J. Davis, in *Advances in Chemical Engineering* (Academic, San Diego, 1992), Vol. 18.
[10] (a) K. H. Fung and I. N. Tang, Appl. Opt. **27**, 206 (1988); (b) J. Colloid Interface Sci. **130**, 219 (1989); (c) Appl. Spectros. **45**, 734 (1991).
[11] K. H. Fung, D. G. Imre, and I. N. Tang, J. Aerosol Sci. **25**, 479 (1994).
[12] E. J. Davis, M. F. Buehler and T. L. Ward, Rev. Sci. Instrum. **61**, 1281 (1990).
[13] M. F. Buehler, T. M. Allen, and E. J. Davis, J. Colloid Interface Sci. **146**, 79 (1991).
[14] W. Li, S. D. Rassat, W. R. Foss and E. J. Davis, J. Colloid Interface Sci. **162**, 267 (1994).
[15] D. E. Irish and M. H. Brooker, in *Advances in Infrared and Raman Spectroscopy*, edited by R. J. H. Clark and R. E. Hester (Heyden, New York, 1976), Vol. 2, p. 212.
[16] M. H. Brooker, in *The Chemical Physics of Solvation*, Part B, edited by R. R. Dogonadze, E. Kalman, A. A. Kornyshev, and J. Ulstrup (Elsevier, Amsterdam, 1986), Chap. 4, p. 119.
[17] I. N. Tang, K. H. Fung, D. G. Imre, and H. R. Munkelwitz, Aerosol Sci. Technol. **23**, 443 (1995).
[18] R. A. Robinson and R. H. Stokes, *Electrolyte Solutions*, 2nd ed. (Butterworths, London, 1970).
[19] I. N. Tang, in *Generation of Aerosols*, edited by K. Willeke (Ann Arbor Science, Ann Arbor, 1980), Chap. 7, p. 153.
[20] M. J. Rood, M. A. Shaw, T. V. Larson, and D. S. Covert, Nature (London) **337**, 537 (1989).
[21] A. Seidell and W. F. Linke, *Solubilities of Inorganic and Metal Organic Compounds*, 4th ed. (Am. Chem. Soc., Washington, D.C., 1965).
[22] M. H. Brooker, D. E. Irish, and G. E. Boyd, J. Chem. Phys. **53**, 1083 (1970).
[23] D. D. Wagman, W. H. Evans, V. B. Parker, R. H. Schumm, and R. L. Nuttall, *Selected Values of Chemical Thermodynamic Properties*, NBS Technical Note 270-8 (U.S. Department of Commerce, 1981).
[24] J. P. Mathieu and M. Lounsbury, Discuss Faraday Soc. **9**, 196 (1950).
[25] J. T. Bulmer, T. G. Chang, P. J. Gleeson, and D. E. Irish, J. Solution Chem. **4**, 969 (1975).
[26] G. Fleissner, A. Hallbrucker, and E. Mayer, J. Chem. Soc. Faraday Trans. **92**, 23 (1996).
[27] R. H. Stokes and R. A. Robinson, J. Am. Chem. Soc. **70**, 1870 (1948).
[28] D. E. Irish, A. R. Davis, and R. A. Plane, J. Chem. Phys. **50**, 2262 (1969).
[29] R. E. Hester and R. A. Plane, J. Chem. Phys. **40**, 411 (1964).
[30] D. E. Irish and G. E. Walrafen, J. Chem. Phys. **46**, 378 (1967).
[31] Y. Marcus, *Ion Solvation* (Wiley, New York, 1985), Chap. 8.
[32] B. Balshaw and S. I. Smedley, J. Phys. Chem. **79**, 1323 (1975).
[33] F. H. Fisher and A. P. Fox, J. Solution Chem. **7**, 561 (1978).
[34] R. Thurn and W. Kiefer, Appl. Opt. **24**, 1515 (1985).
[35] G. E. Rodgers and R. A. Plane, J. Chem. Phys. **63**, 818 (1975).
[36] C. I. Ratcliffe and D. E. Irish, J. Phys. Chem. **86**, 4897 (1982).
[37] G. E. Walrafen, in *Structure of Water and Aqueous Solutions*, edited by W. A. P. Luck (Verlag Chemie, Weinheim, 1974).
[38] J. R. Scherer, in *Advances in Infrared and Raman Spectroscopy*, edited by R. J. H. Clark and R. E. Hester (Heyden, London, 1978), Vol. 5, Chap. 3.
[39] J. L. Green, A. R. Lacey, and M. G. Sceats, J. Phys. Chem. **90**, 3958 (1986).